Segregation of Receptive Field Properties in the Lateral Geniculate Nucleus of a New-World Monkey, the Marmoset *Callithrix jacchus*

ANDREW J. R. WHITE, HEATH D. WILDER, ANN K. GOODCHILD, ANN JERVIE SEFTON, AND PAUL R. MARTIN

Department of Physiology and Institute for Biomedical Research, The University of Sydney, New South Wales 2006, Australia

White, Andrew J. R., Heath D. Wilder, Ann K. Goodchild, Ann Jervie Sefton, and Paul R. Martin. Segregation of receptive field properties in the lateral geniculate nucleus of a New-World monkey, the marmoset *Callithrix jacchus*. *J. Neurophysiol.* 80: 2063–2076, 1998. The lateral geniculate nucleus (LGN) in humans and Old-World monkeys is dominated by the representation of the fovea in the parvocellular (PC) layers, and most PC cells in the foveal representation have red–green cone opponent receptive field properties. It is not known whether these features are both unique to trichromatic primates. Here we measured receptive field properties and the visuotopic organization of cells in the LGN of a New-World monkey, the marmoset *Callithrix jacchus*. The marmoset displays a polymorphism of cone opsins in the medium-long wavelength (ML) range, which allows the LGN of dichromatic (''red–green color blind'') and trichromatic individuals to be compared. Furthermore, the koniocellular–interlaminar layers are segregated from the main PC layers in marmoset, allowing the functional role of this subdivision of the LGN to be assessed. We show that the representation of the visual field in the LGN is quantitatively similar in dichromatic and trichromatic marmosets and is similar to that reported for macaque; the vast majority of LGN volume is devoted to the central visual field. ON- and OFF-type responses are partially segregated in the PC layers so that ON responses are more commonly encountered near the external border of each layer. The red–green (ML) opponent cells in trichromatic animals were all located in the PC layers, and their receptive fields were within 16° of the fovea. The koniocellular zone between the PC and magnocellular layers contained cells that receive excitatory input from short wavelength sensitive cones (''blue-ON cells'') as well as other nonopponent cells. These results suggest that the basic organization of the LGN is common to dichromatic and trichromatic primates and provide further evidence that ML and SWS opponent signals are carried in distinct subdivisions of the retinogeniculocortical pathway.

INTRODUCTION

The lateral geniculate nucleus (LGN) of anthropoid primates is normally described as consisting of two major subdivisions, the parvocellular (PC) layers and the magnocellular (MC) layers, separated by sparsely populated interlaminar or koniocellular zones. The bulk of the LGN in these species is devoted to the representation of the foveal retina in the PC layers (Connolly and Van Essen 1984; Le Gros Clark 1941; Malpeli and Baker 1975; Walls 1953). The PC layers have also been associated with the cone opponent responses underlying trichromatic color vision (Derrington et al. 1984; Dreher et al. 1976; Schiller and Colby 1983; Schiller and Malpeli 1978; Wiesel and Hubel 1966). It has been argued that these two features of the primate visual system are interlinked so that the retinal specialization for high spatial resolution foveal vision was a necessary precursor to the evolution of trichromatic color vision (Lennie et al. 1991; Wässle and Boycott 1991).

The laminated structure of the LGN is also associated with a segregation of ON- and OFF-center receptive fields in several mammalian species [mink (Le Vay and McConnell 1982), tree shrew (Conway and Schiller 1983; Holdefer and Norton 1995), and ferret (Stryker and Zahs 1983)], but evidence for such segregation in the LGN of Old-World primates was so far negative [*Galago* (Norton and Casagrande 1982)] or equivocal [macaque (Derrington and Lennie 1984; Kaplan and Shapley 1986; Schiller and Malpeli 1978; Wiesel and Hubel 1966)].

We addressed these questions by comparing the functional organization of the LGN in animals with dichromatic (''red–green color blind'') and trichromatic color vision. In common with most other New-World monkeys, the common marmoset (*Callithrix jacchus*) displays a polymorphism of color vision (Jacobs 1983, 1996; Jacobs et al. 1996; Mollon et al. 1984; Tovée et al. 1992; Travis et al. 1988; Williams et al. 1992) so that both dichromatic and trichromatic individuals are present (Hunt et al. 1993; Jacobs 1983; Yeh et al. 1995b). The males express a short-wavelength sensitive (SWS) cone pigment and one of three alleles of medium-long wavelength (ML) sensitive pigments, which occupy the same locus on the X chromosome. Heterozygous females, which can express two of these three ML-sensitive pigments, demonstrate behavioral signs of trichromacy (Tovée et al. 1992; Williams et al. 1992). The retina and subcortical visual pathways in marmosets are similar to those described for Old-World primates in both their anatomic (Ghosh et al. 1996; Troilo et al. 1993; Wilder et al. 1996; Yamada et al. 1996) and receptive field properties (Kremers et al. 1997; Martin et al. 1997; Yeh et al. 1995b). The spatial density and connectivity of photoreceptors and ganglion cells in the fovea of the marmoset are quantitatively similar to those in macaque and human (Curcio et al. 1990; Wässle et al. 1989; Wilder et al. 1996), meaning that the species can serve as a useful model for diurnal primate vision.

We made extracellular single cell recordings in the mar-

The costs of publication of this article were defrayed in part by the payment of page charges. The article must therefore be hereby marked ''*advertisement*'' in accordance with 18 U.S.C. Section 1734 solely to indicate this fact.

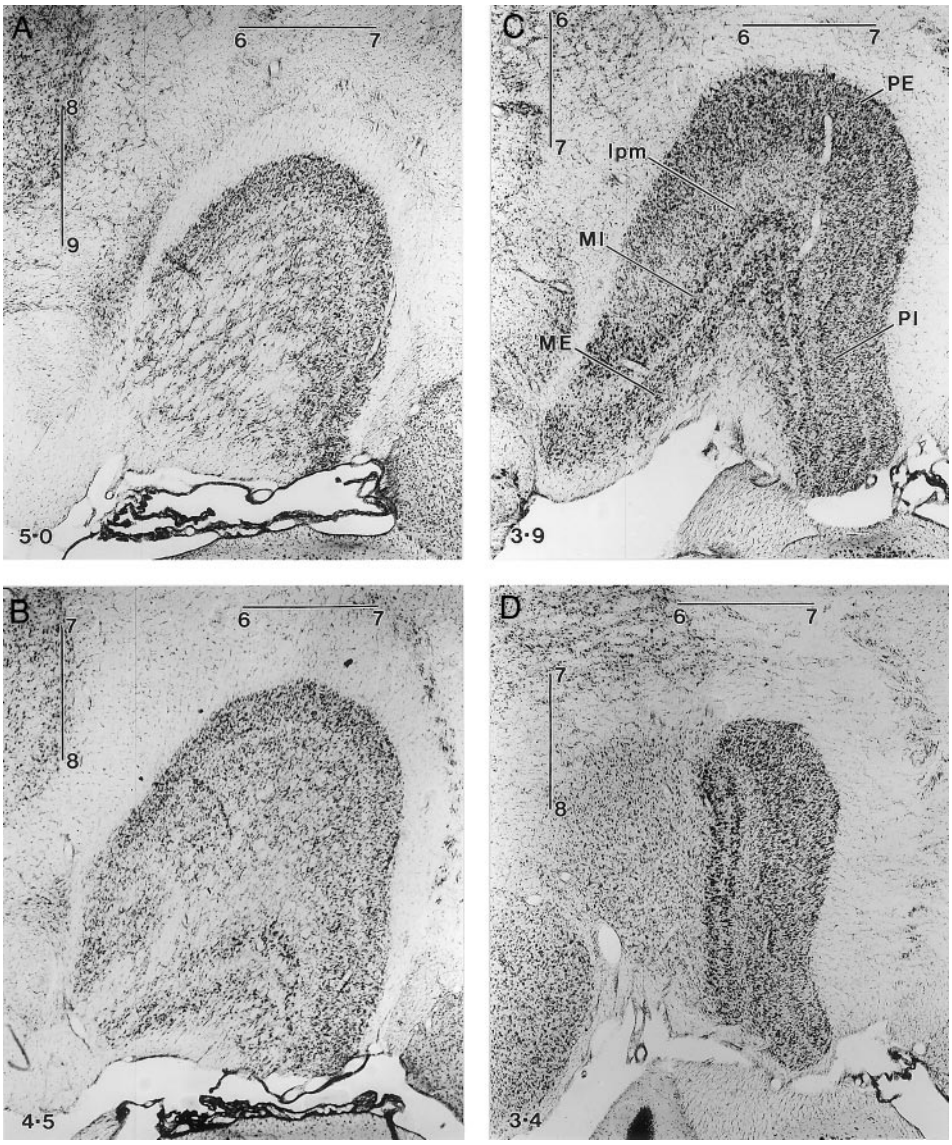

FIG. 1. Coronal sections through the lateral geniculate nucleus (LGN) of a female marmoset at 4 different locations from anterior (*A*) to posterior (*D*). Cresyl violet stain. Distance (mm) from the interaural axis is shown at the *bottom left* of each photomicrograph. Magnocellular layers are not present in the most anterior section (*A*). All layers can be distinguished most readily in sections through the posterior one-half of the LGN (*C* and *D*). Nomenclature according to Kaas et al. (1978). PE, external parvocellular (PC) layer; PI, internal PC layer; Ipm, interlaminar zone; MI, internal magnocellular (MC) layer; ME, external MC layer. The vertical and horizontal bars in each photomicrograph are 1 mm long. They show distance (in mm) from the midline and depth (in mm) below the surface of the cortex. Section thickness 30 μm.

moset LGN. We then reconstructed histologically the LGN to attribute receptive field properties to specific layers of the nucleus. We demonstrate that, in both dichromatic and trichromatic animals, the LGN is dominated by the foveal representation. There is a mild segregation of ON- and OFF-response properties according to depth within the PC layers. In trichromatic animals, the ML opponent cells are restricted to the PC layers in the foveal representation, but they are not segregated according to depth within the layers. The results argue for the existence of a common mechanism of response segregation in the LGN of dichromatic and trichromatic primates and are consistent with the hypothesis that the presence of the fovea and its central representation was a prerequisite for the evolution of trichromatic color vision.

METHODS

Physiological measurements

Recordings were made from 10 adult marmosets (*Callithrix jacchus*), body weight 250–370 g. Animals were obtained from the Australian Commonwealth Scientific and Industrial Research Organization/National Health and Medical Research Council of Australia combined breeding facility in Adelaide. Three of the animals were male; the others were female. In this study we describe in detail the results obtained from seven female animals from which complete anatomic reconstructions of the LGN were made. All procedures used are approved by the University of Sydney Institutional Animal Care and Ethics committee and conform with the provisions of the Australian NHMRC code of practice for the care and use of animals. The animals were anesthetised with a mixture of xylazine (~0.3 mg/kg im) and ketamine (30 mg/kg im) for surgery. Anesthesia was maintained with isoflurane (2% during surgical procedures, 0.25–0.75% during recording) and a 70%-30% mixture of NO_2:carbogen (5% CO_2 in O_2). A venous infusion of 40 $\mu g \cdot kg^{-1} \cdot h^{-1}$ alcuronium chloride (Alloferin, Roche) in dextrose Ringer solution was infused at a rate of 1 ml/h to maintain muscular relaxation. Electroencephalogram and electrocardiogram signals were monitored to ensure adequate depth of anesthesia; in some experiments arterial blood pressure was also monitored by way of a femoral catheter. End-tidal CO_2 was measured and maintained near 4% by adjusting the rate and stroke volume of the inspired gas mixture. The pupils were dilated with topical neosynephrine (10%). Penicillin and corticosteroids were administered daily.

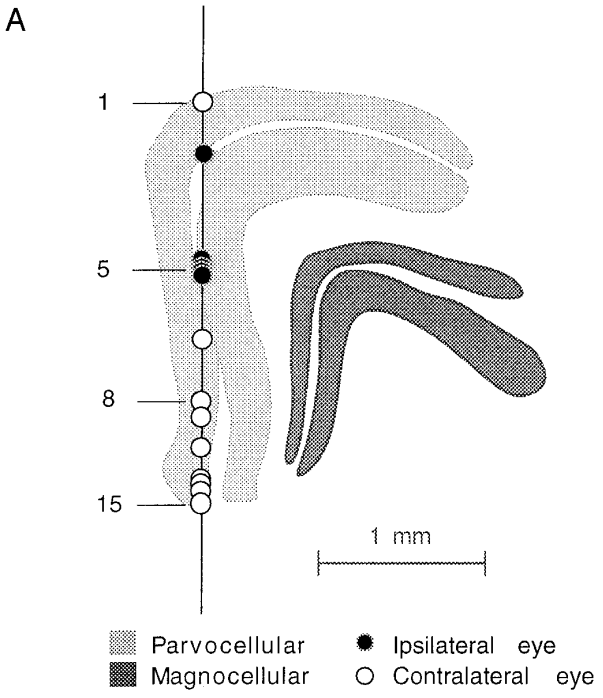

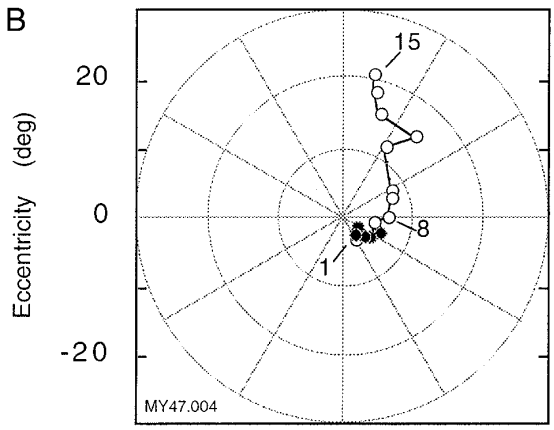

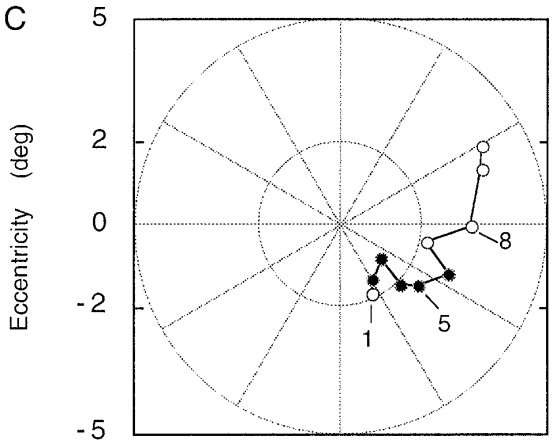

The animal was mounted in a stereotaxic headholder. The eyes were protected with oxygen-permeable contact lenses and focused on a tangent screen at a distance of 114 cm with supplementary lenses if required. The stereotaxic frame was tilted to bring the optic axis close to the horizontal plane, and the locations of the fovea and optic disk were mapped onto the tangent screen with the aid of a fundus camera equipped with a rear projection device. The table supporting the stereotaxic frame could be rotated as required to bring the receptive fields of recorded cells close to the center of the tangent screen. Such movements were monitored by means of a laser attached to the table.

A craniotomy was made over the LGN and a microelectrode (parylene-coated tungsten or glass-coated steel; impedance 5–12 MΩ, F. Haer, Brunswick, ME) was lowered into the LGN. Action potentials arising from single cells were identified, and the time of their occurrence was measured with an accuracy of 0.1 ms and stored. The visual receptive field location of the multiunit ''swish'' was also measured at regular intervals throughout the electrode penetration; these measurements were used together with single cell receptive fields to derive the visuotopic map of the LGN.

Visual stimuli

Each visually responsive cell was initially classified by using hand-held stimuli; thereafter all stimuli were delivered through a Maxwellian view system (Smith et al. 1992; Yeh et al. 1995b), which was aligned along the axis of each cell's receptive field and centered on the pupil of the eye. The stimulus in the plane of the pupil was a spatially uniform field composed of the combined image of red, green, and blue light-emitting diodes (LEDs). Temporal waveforms were generated through 12-bit DA converters (NB-A06, National Instruments) under computer control. The LED driver circuitry (Swanson et al. 1987) ensured a linear relationship between driving voltage and LED intensity. The stimulus was calibrated with a PR-650 spectrophotometer (Photo Research, CA). The LED dominant wavelengths were 639, 554, and 470 nm; bandwidth <20 nm at one-half height. An 8-mm aperture was normally placed at the rear focal plane of the Maxwellian view lens to give a stimulus subtense of 6.4°. An artificial pupil was not used. The areal image of the 8-mm aperture was smaller than the diameter of the dilated pupil and thus formed the exit aperture of the optical system. Time-averaged illuminance (measured according to Westheimer 1966) for the red and green LEDs combined was ~1,000 Photopic Trolands; the smaller size of the marmoset eye (Troilo et al. 1993) means that retinal flux per Troland is almost four times higher than for human. Stimuli were normally unattenuated as we wished to minimize the possibility of rod intrusion, which was seen at relatively high levels of retinal illuminance by Yeh et al. (1995b) and Kremers et al. (1996). For some OFF-center cells, responsivity was significantly improved when the stimulus was attenuated by 1 ND.

Responses to at least three stimulus paradigms were used to classify cell types. Each paradigm was based on a 4.1-s stimulus epoch and was designed to probe one aspect of the cell's performance within the shortest possible recording time. In the first stimulus paradigm, a measure of cell responsiveness to luminance con-

FIG. 2. Retinotopic progression in marmoset LGN. *A*: camera lucida drawing of the LGN with the reconstructed path of a recording electrode. Location of each cell encountered on the path is indicated. *B*: receptive field location of cells encountered in this path. Each point shows the center of the receptive field. Open symbols, cells driven by ipsilateral eye; closed symbols, cells driven by contralateral eye. *C*: same map on an enlarged scale to show the progression of receptive fields near the foveal representation. Receptive fields of cells located at progressively more ventral locations in the lateral aspect of the LGN show a systematic displacement to greater elevations in the visual field.

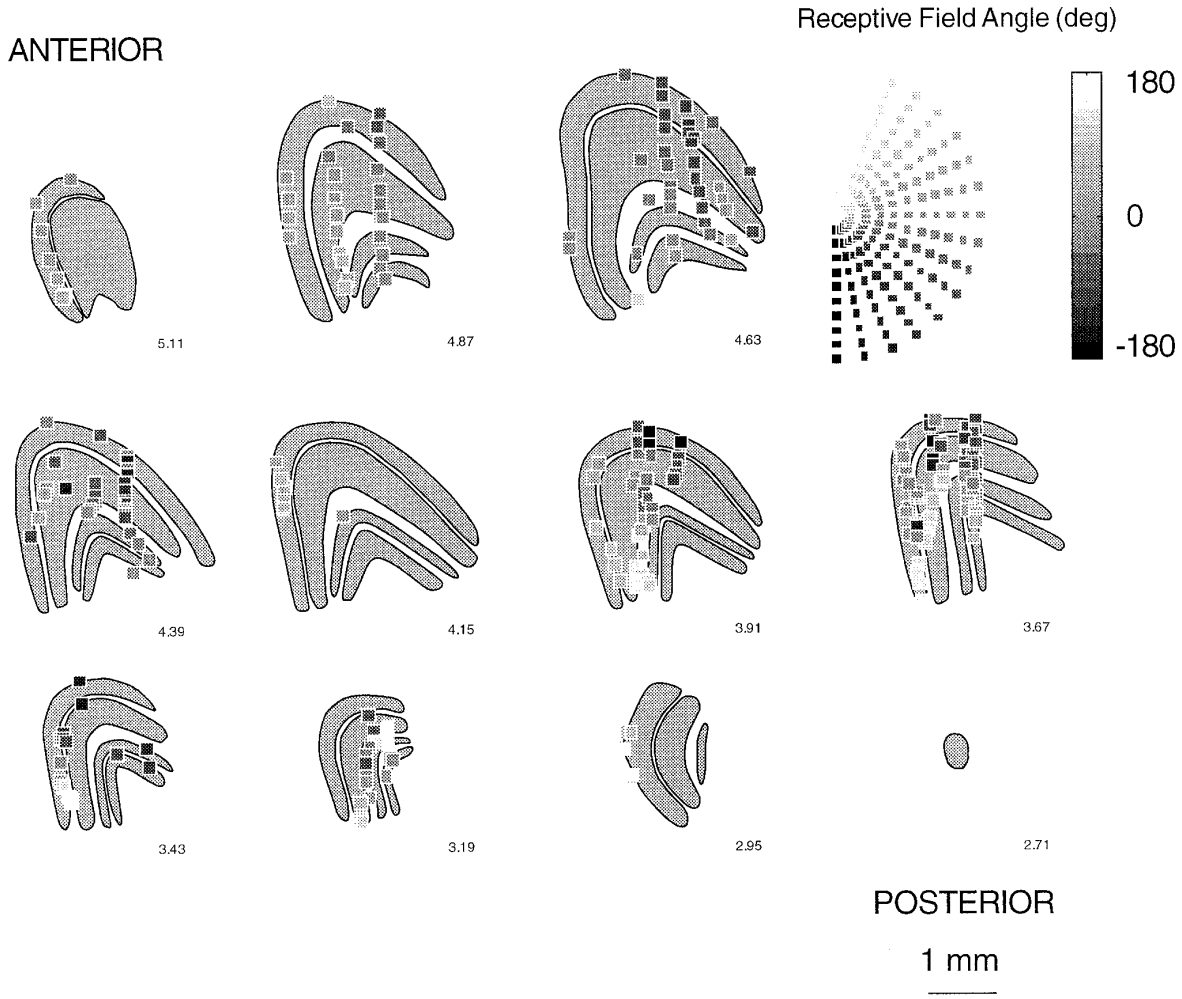

FIG. 3. Composite drawings of the LGN at different coronal levels, showing the location of recorded cells (small squares). Each square is assigned a gray level according to the angle of its receptive field location with respect to the fovea, as indicated by the key diagram at *top right*. Upper field locations (lighter gray) are located in the lateral aspect of the LGN, and lower field locations (darker gray) are located in the medial aspect of the LGN.

trast was made by modulating the red and green LEDs in phase at 3.906 Hz. Contrast was varied with a sine envelope over the stimulus epoch. In a second paradigm, responsivity to red–green chromatic contrast was measured in the same way, except that the red and green LEDs were modulated out of phase. In the third stimulus paradigm the blue and red LEDs were combined and modulated out of phase with the green LED, with their relative amplitudes adjusted to provide differential excitation to SWS cones (Yeh et al. 1995a). The maximum luminance available from the blue LED was 7% that of the red or green, so for this paradigm the red and green amplitude were reduced accordingly. Modulation was between CIE $x, y = 0.3, 0.13$ and $x, y = 0.46, 0.521$. The modulation depth of the LED was usually set at 100%. Where the responses showed significant saturation, measurements were also made at 50 or 25% modulation depth.

Tissue preparation

The location of each recorded cell was noted by reading the depth from the hydraulic microelectrode advance (David Kopf Model 640). Electrolytic lesions (6–20 μA $\times$ 10–20 s, electrode negative) were made at the location of some cells. At least two lesions were made on each electrode track. If a steel recording electrode was used, some locations were marked by passing positive current for later reaction by the Prussian blue method. At the end of the recording session the animal was killed with an overdose of pentobarbitone sodium (80–150 mg/kg iv) and perfused with intracardially with saline (0.9% NaCl, 0.4 l) followed by freshly prepared 4% paraformaldehyde in 0.1 M phosphate buffer (PB; pH 7.4., 0.5 l) with 10% potassium ferrocyanide. The brain was removed and placed in 30% sucrose in PB until it sank. Serial coronal sections at 30-μm thickness were cut on a freezing microtome, mounted, air dried, stained with cresyl violet, dehydrated, and coverslipped with Ultramount.

Analysis

The analysis was made at two levels of precision. The visuotopic map was established from both single and multiple unit recording sites throughout the LGN. A subset of these recording positions also satisfied the following criteria. The action potential was identified as arising from a single cell body (Bishop et al. 1962), the responses of the cell to all three stimulus paradigms described above were measured, and the histological construction allowed the position of the cell to be determined with respect to the laminar borders within the LGN. These cells formed the database for the descriptions of single cell properties.

The location of recorded cells was established by first tracing

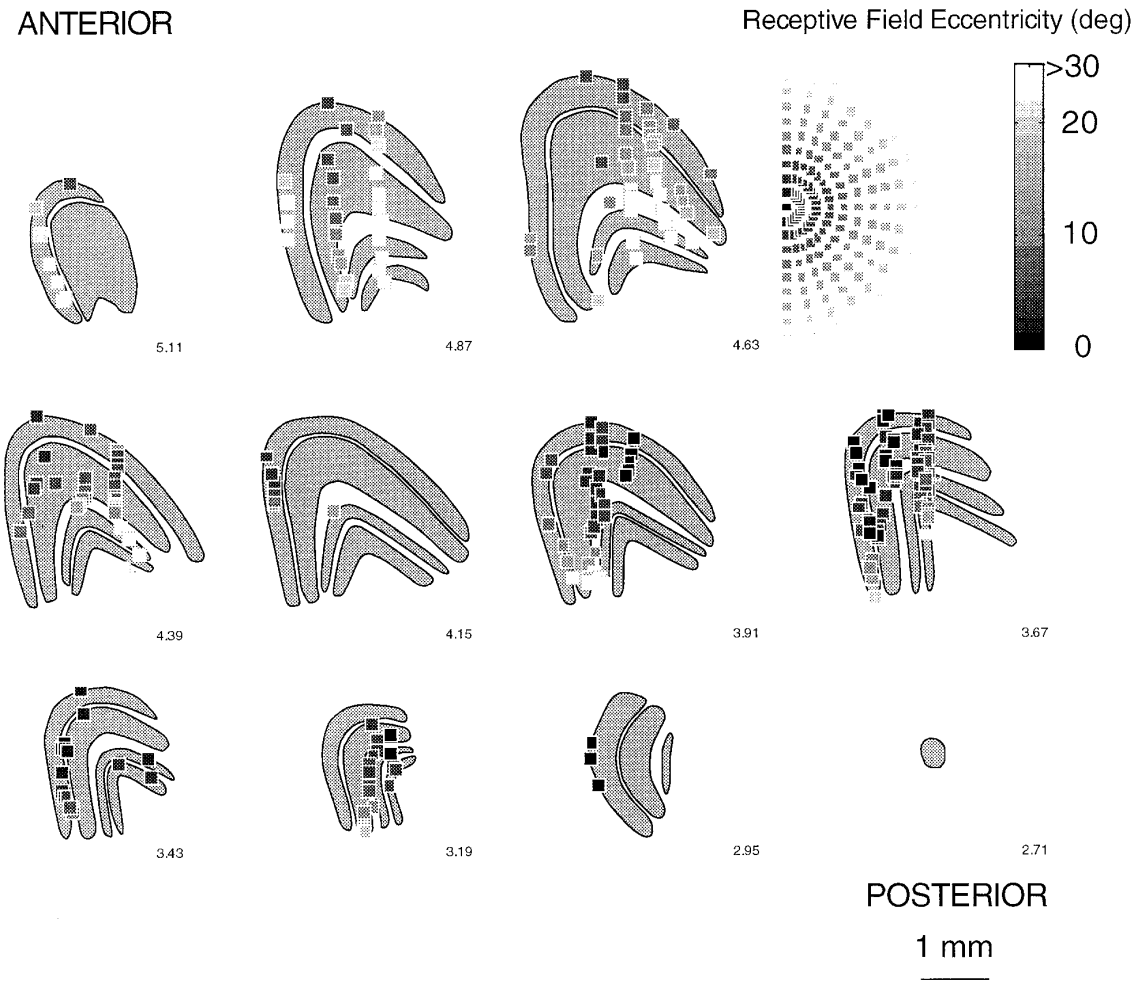

FIG. 4. This figure has the same format as Fig. 3. The gray scale shows receptive field eccentricity with respect to the fovea. Fovea is represented in the posterodorsal aspect of each layer of the LGN.

the outline of the LGN laminae from cresyl violet stained sections, after which each electrode track was reconstructed by identifying lesions or blue marker spots. For many tracks the electrode trajectory could also be identified by localized tissue damage. Tissue shrinkage was estimated by measuring the distance between lesions and comparing this value with the reading from the micropositioner. Shrinkage was ~12% (linear). The location of each recorded cell was marked on the drawing. The depth within the lamina and angle with respect to the genu of the LGN were measured for each cell. A map of representative LGN sections was drawn to compare results from different animals. The location of each cell was plotted onto this standard set of laminar coordinates. Measurements of laminar area were made from scanned images of these drawings and from published maps of LGN topography in macaque (Connolly and Van Essen 1984) with NIH image software. We use the nomenclature of Kaas et al. (1978) for the LGN laminae.

The amplitude and phase of cell responses were measured by Fourier analysis of spike density. Amplitude values are taken from the Fourier component at the frequency of modulation of the red LED.

RESULTS

Morphology of the marmoset LGN

Figure 1 shows representative coronal sections through the marmoset LGN. The basic lamination pattern of two PC and two MC layers separated by an interlaminar zone with small cell bodies (Kaas et al. 1978; Spatz 1978) is most easily seen in the posterior aspect of the LGN (Fig. 1*C*). In more anterior sections (Fig. 1*A*) the MC layers are not present. The stereotaxic coordinates indicated for this brain on Fig. 1 are in good agreement with the LGN coordinates from the atlas of the marmoset brain (Stephan et al. 1980). Although there was some variability among animals, we found that electrode penetrations at coordinates anteroposterior 4.0, lateral 6.5 usually passed through the central visual field representation in the LGN. No clear difference in the size or lamination pattern of the LGN was seen between male and female marmosets or between females identified as dichromatic or trichromatic in the recording experiment.

Visual field representation

We first confirmed the observation of Yeh et al. (1995b) that the visual field map of macaque LGN (Malpeli and Baker 1975) gives a reasonable guide to retinotopic organization in the marmoset LGN. Cells with foveal receptive fields were encountered in penetrations in the posterodorsal aspect of the LGN, with progressively peripheral locations represented in anterior and ventral locations. The progression

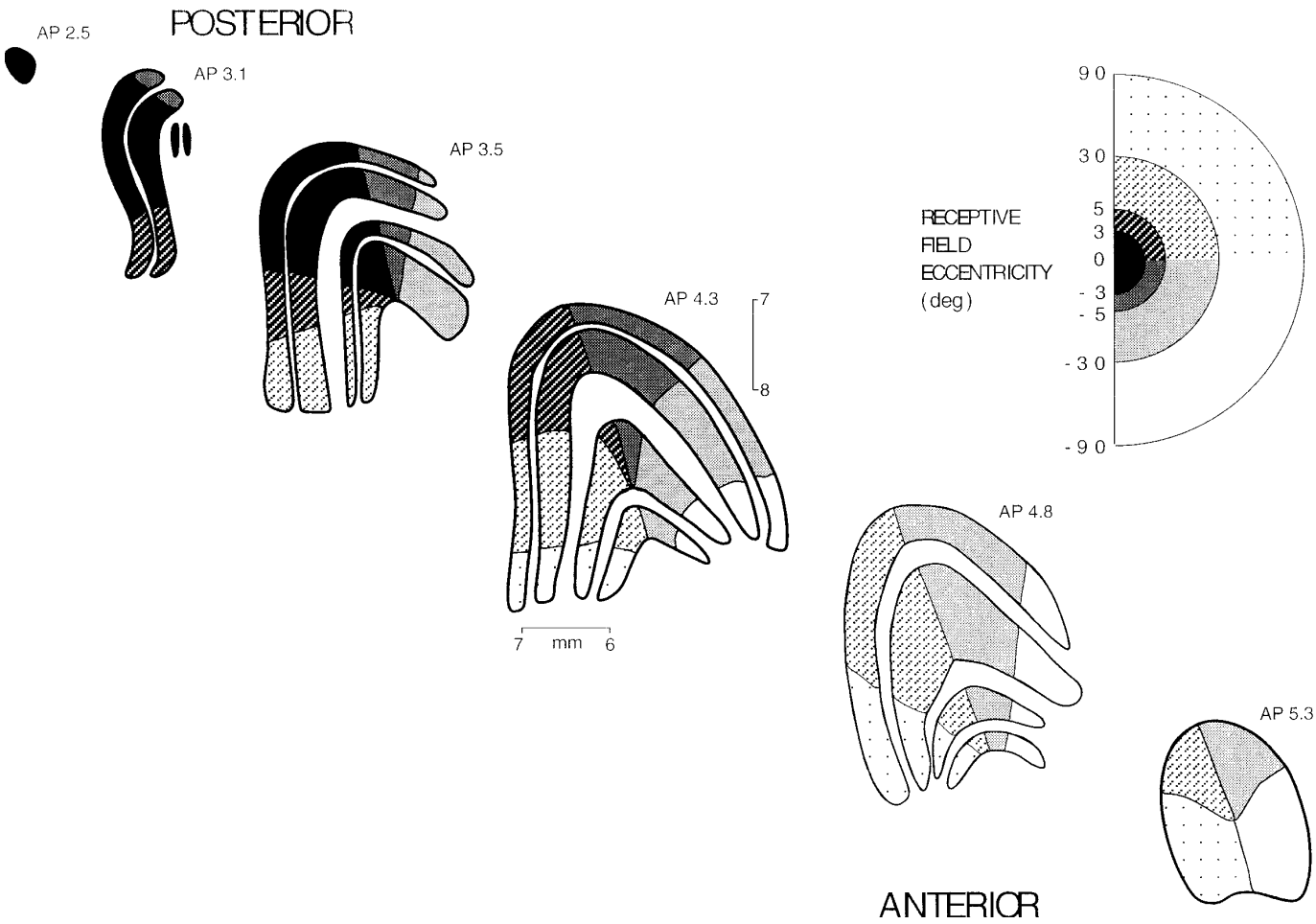

FIG. 5. Summary drawing of the visuotopic map in the marmoset LGN, based on the data shown in Figs. 3 and 4. Visual field zones and their representation in the LGN are shown in different hatch patterns. Anteroposterior distance from the interaural axis (in mm) is indicated above each representative coronal section. Only the PC layers are present at AP level 5.3 mm. Scale bars (1 mm) also show distance from the midline and depth below the cortex (mm) for 1 section.

of receptive field location and eye allegiance for a typical penetration is shown in Fig. 2. As for the macaque (Malpeli and Baker 1975; Malpeli et al. 1996), a line running from the hilum to the genu of the LGN marks the representation of the horizontal meridian. The dorsal visual field is represented on the lateral aspect of the LGN (Fig. 2*C*, *cells 8–13*), and the ventral field is represented on the medial aspect of the LGN. The contralateral eye almost always provided the dominant excitatory drive for cells located in the external PC and the internal MC layers. Cells in the internal PC and external MC layers and the majority of cells in the koniocellular zone between the MC and PC layers were driven by the ipsilateral eye. In penetrations through the posterior LGN (foveal representation), we occasionally encountered one or two cells within a lamina that were driven by the ''wrong'' eye. Their location may correspond to the laminar leaflets revealed by autoradiographic tracing studies in this species (Kaas et al. 1978; Spatz 1978). The electrode path in the ventral part of the LGN was sometimes slightly curved. As reported for macaque by Malpeli et al. (1996), this may be a result of unequal shrinkage.

We next made a quantitative evaluation of the visual field representation in the marmoset LGN. In the composite maps shown in Figs. 3 and 4, we indicate the location of 280 recording sites (single and multiunit recordings) within the LGN recorded in seven female animals (4 dichromats, 3 trichromats), with receptive field angle (Fig. 3) and distance from the fovea (Fig. 4) coded by gray scale. The orientation of the retinotopic map in each layer is preserved with upper fields on the lateral and lower fields on the medial aspect of the LGN and the foveal representation located posterodorsally within each layer. On the basis of these data a set of lines was drawn at each anteroposterior level to encompass receptive field locations within four zones of the visual field: 0–3°, 3.1–5°, 5.1–30°, and >30°. These subdivisions are shown in Fig. 5. The small volume of the MC layers relative to the PC and the possibility of nonuniform shrinkage meant that relatively few cells were encountered there, so the map cannot be determined as accurately for the magnocellular layers. Nevertheless, >85% of recorded receptive fields in all layers lie within the borders shown. No systematic differences in the visuotopic organization were seen when the dichromatic and trichromatic animals were compared.

Foveal magnification

We measured the volume of the LGN that is devoted to each of the visual field zones shown in Fig. 5. For each

TABLE 1. *LGN volume and visual field representation*

Zone	1	2	3	4	Total
Eccentricity range, deg	0–3	3.1–5	5.1–30	>30	
Volume, mm^3					
PE	0.897	1.173	1.619	1.559	5.248
PI	0.832	1.371	1.593	0.754	4.550
ME	0.150	0.292	0.785	0.357	1.584
MI	0.215	0.116	1.043	0.346	1.720
PC (PE + PI)	1.729	2.544	3.212	2.313	9.798
MC (ME + MI)	0.365	0.408	1.828	0.703	3.304
Total	2.094	2.952	5.040	3.016	13.102
Total volume, %					
PC	13.200	19.400	24.500	17.700	74.800
MC	2.800	3.100	13.900	5.400	25.200
PC + MC	16.000	22.500	38.400	23.100	100.000
Ratio PC/MC	4.714	6.258	1.763	3.278	4.003
Macaque total volume, %					
PC*	6.500	10.200	44.900	18.800	80.400
MC*	0.700	1.900	9.300	7.700	19.600
PC + MC*	7.200	12.100	54.200	26.500	100.000
LGN†	13.636	9.643	52.176	24.545	100.000
Ratio PC/MC*	9.286	5.368	4.828	2.442	4.102

LGN, lateral geniculate nucleus; PE, external parvocellular (PC) layer; PI, internal PC layer; ME, external magnocellular (MC) layer; MI, internal MC layer. * Connolly and van Essen 1984. † Malpeli and Baker 1975.

lamina, the area within each zone was measured. The volume for each zone was calculated with Cavalieri's method (Gundersen and Jensen 1987). Table 1 shows that the PC layers make up ~75% of the total laminar volume of the LGN. The total laminar volume of the marmoset LGN (13.09 mm^3) is about one-fifth the volume of macaque LGN (65–70 mm^3) (Ahmad and Spear 1993; Malpeli et al. 1996). These values are consistent with estimates of the overall dimensions of the LGN: macaque, 3.75 mm (anteroposterior) × 4.9 mm (mediolateral) × 4.8 mm (dorsoventral) by Le Gros Clark (1941; see also Connolly and van Essen 1984) and marmoset 3.0 mm (anteroposterior) × 2.9 mm (mediolateral) × 2.8 mm (dorsoventral) (our data; see also Kaas et al. 1978; Spatz 1978). The total LGN volume in macaque is 88.2 mm^3, and in marmoset the total LGN volume is 24.6 mm^3. The ratio of these volumes is 3.6:1.

We also made measurements from the reconstructed visual field map of macaque LGN made by Connolly and Van Essen (1984, their Fig. 8) from Malpeli and Baker's (1975) data. The area of each lamina devoted to each visual field zone was measured from their drawing and multiplied by the thickness of each lamina to give laminar volume. These values are shown in Table 1. A similar calculation for the entire LGN (including interlaminar zones) from Malpeli and Baker (1975, p. 587) is also shown. For both macaque and marmoset, >75% of the nucleus is devoted to the representation of the central 30°, and there is an increase in the ratio of PC to magnocellular volume within the central 5°. The results show that, in quantitative as well as qualitative terms, the visual field representation in the LGN is similar in the marmoset and macaque.

Segregation of ON and OFF responses

The first cell encountered in any given electrode penetration usually had an ON-center receptive field. For 27 penetrations, 80% of the first cells encountered in the external PC layer were ON-center cells. We measured the laminar position of cells classified as ON- or OFF- center, both from the response to hand-held stimuli and from the phase of the cells' responses to luminance modulation. Cells showing evidence of input from SWS cones were excluded from this analysis. The results are shown in Fig. 6. There is a slight preponderance of ON-center cells over OFF-center cells in both the PC and magnocellular layers, as reported for macaque (Derrington and Lennie 1984; Kaplan and Shapley 1986; Schiller and Malpeli 1978; Wiesel and Hubel 1966). There is also a segregation within the PC laminae, so that ON-center cells are more frequently encountered in the external part of each PC layer and OFF responses predominate in the internal one-half of each layer. The difference between the internal and external one-half of each layer is statistically significant for the PC layers (Mann-Whitney $U = 3127.5$, $P = 0.0048$). No such segregation is apparent for the magnocellular layers (Mann-Whitney $U = 159.5$, $P = 1$) nor was a clear difference apparent for dichromatic or trichromatic animals.

Distribution of ML cone opponent cells

We examined the distribution of cone opponent response properties within the marmoset LGN. Figure 7 shows examples of cells receiving input from cone mechanisms in the ML range. The responses of two PC cells and one magnocellular cell are compared. Two stimulus paradigms are shown, luminance modulation (Fig. 7*A*) and equal luminant red–green chromatic modulation (Fig. 7*B*). The amplitude of the 3.906-Hz Fourier component of each cell's response is shown in Fig. 7*C*. The majority of PC cells and all magnocellular cells were more responsive to luminance than to chromatic modulation. The results are similar to those described by Yeh et al. (1995b); in both macaque and marmoset, MC cells have a steeper contrast-response relationship than PC cells, and response saturation is evident at high contrast

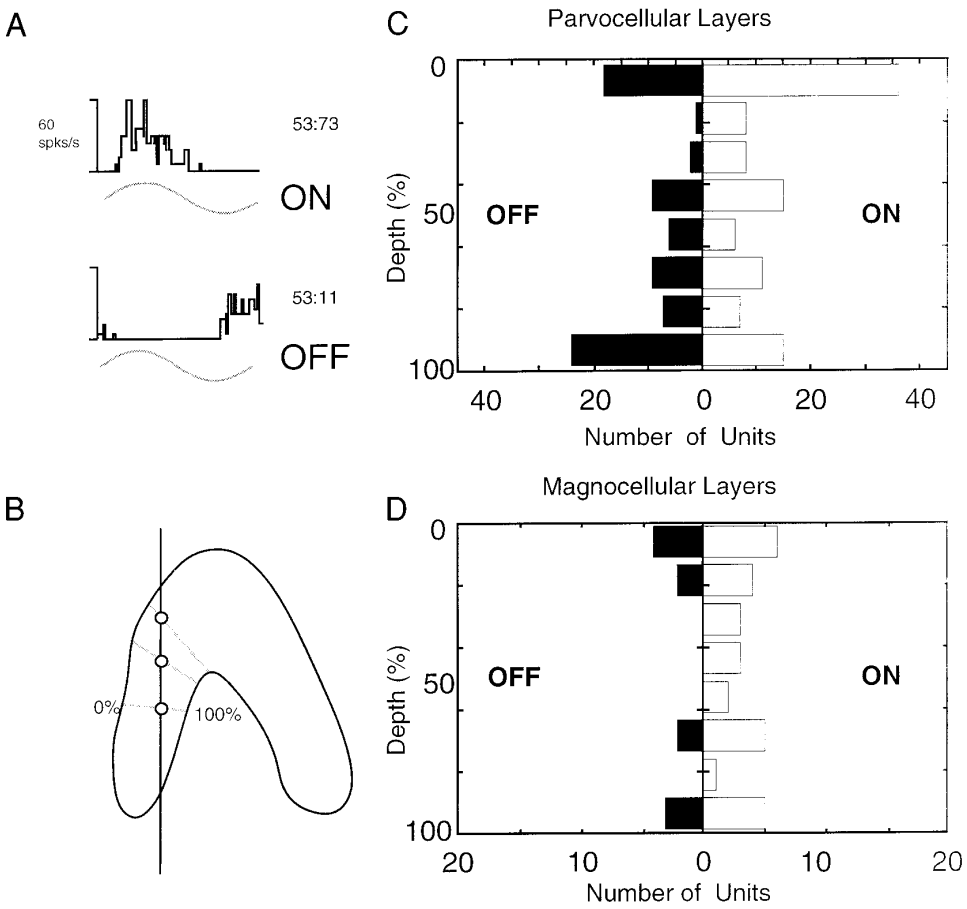

FIG. 6. Distribution of ON and OFF responses within the PC and MC layers. *A*: peristimulus time histograms of the response of 1 ON cell and 1 OFF cell to sinusoidal luminance (in-phase) modulation of red and green LEDs at 3.906 Hz. *B*: schematic outline of 1 LGN lamina. Location of each cell (open circles) in a given electrode track (vertical line) was measured with respect to the laminar borders (gray lines). *C* and *D*: histograms to show the number of ON and OFF cells encountered within 25% depth ranges within the PC (*C*) and MC (*D*) laminae.

levels for MC cells. (Blakemore and Vital-Durand 1986; Derrington and Lennie 1984; Hicks et al. 1983; Kaplan and Shapley 1986).

In three female marmosets, a minority of PC cells was clearly more responsive to red–green chromatic modulation than to luminance modulation (Fig. 7, *row 2*). No such ML opponent responses were seen outside the central 16° of the visual field. Even in the central 10°, overtly opponent and nonopponent PC receptive fields were often encountered with centers separated by <1°. A similar result was reported by Yeh et al. (1995b), who showed a high proportion of nonopponent cells in trichromatic females. This result is different from the situation in macaque, in which the vast majority of PC cells show cone opponency when tested with appropriate stimuli (De Monasterio et al. 1975; Derrington et al. 1984; Padmos and Van Norren 1975).

The MC cells (e.g., Fig. 7, *row 3*) typically showed a small response to equiluminant RG modulation at high contrast levels. These residual responses can be attributed to the derivation of the spectral sensitivity function of marmosets from the human luminosity function (Yeh et al. 1995b). In trichromatic animals, it can also be attributed to the nonlinearity of cone summation in MC projecting cells (Lee et al. 1989a; Yeh et al. 1995b). The MC cells will not be considered further here.

We recorded from 65 cells in the interlaminar zones. A small number (13) were blue-ON cells. The rest showed heterogeneous response properties. No clear signs of ML cone opponency were seen, but at high contrast levels some interlaminar zone cells resembled MC cells; they showed a saturated response to luminance contrast and a strong residual response to equiluminant red–green modulation.

Figure 8 summarizes the distribution of ML opponent responses in the PC layers and interlaminar zones of the marmoset. Figure 8*A* shows for each cell the relative amplitude of response to luminance (LUM) and red–green (RG) modulation as a function of the laminar position. The interlaminar zone cells that showed significant response saturation were excluded from this analysis. Although the total cell sample from trichromatic animals is relatively small, there is a clear tendency for opponent responses to be associated with the central retina (Fig. 8*B*). Within 10° of the fovea, about one-half the PC cells in trichromatic animals (7/13) respond more vigorously to RG than to LUM modulation, whereas at greater eccentricities this proportion is much smaller (1/10). The interlaminar zone cells all show relatively poor responses to RG modulation, reinforcing the observation that in marmoset (Yeh et al. 1995b) as for macaque (Derrington et al. 1984; Dreher et al. 1976; Wiesel and Hubel 1966) ML opponent responses are restricted to the PC layers of the LGN.

Responses and distribution of blue-ON cells

Yeh et al. (1995b) reported the presence of cells receiving input from SWS cones in marmoset LGN but did not characterize these cells further. In this study a small number of cells ($n = 13$) was identified as blue-ON by their responses to hand-

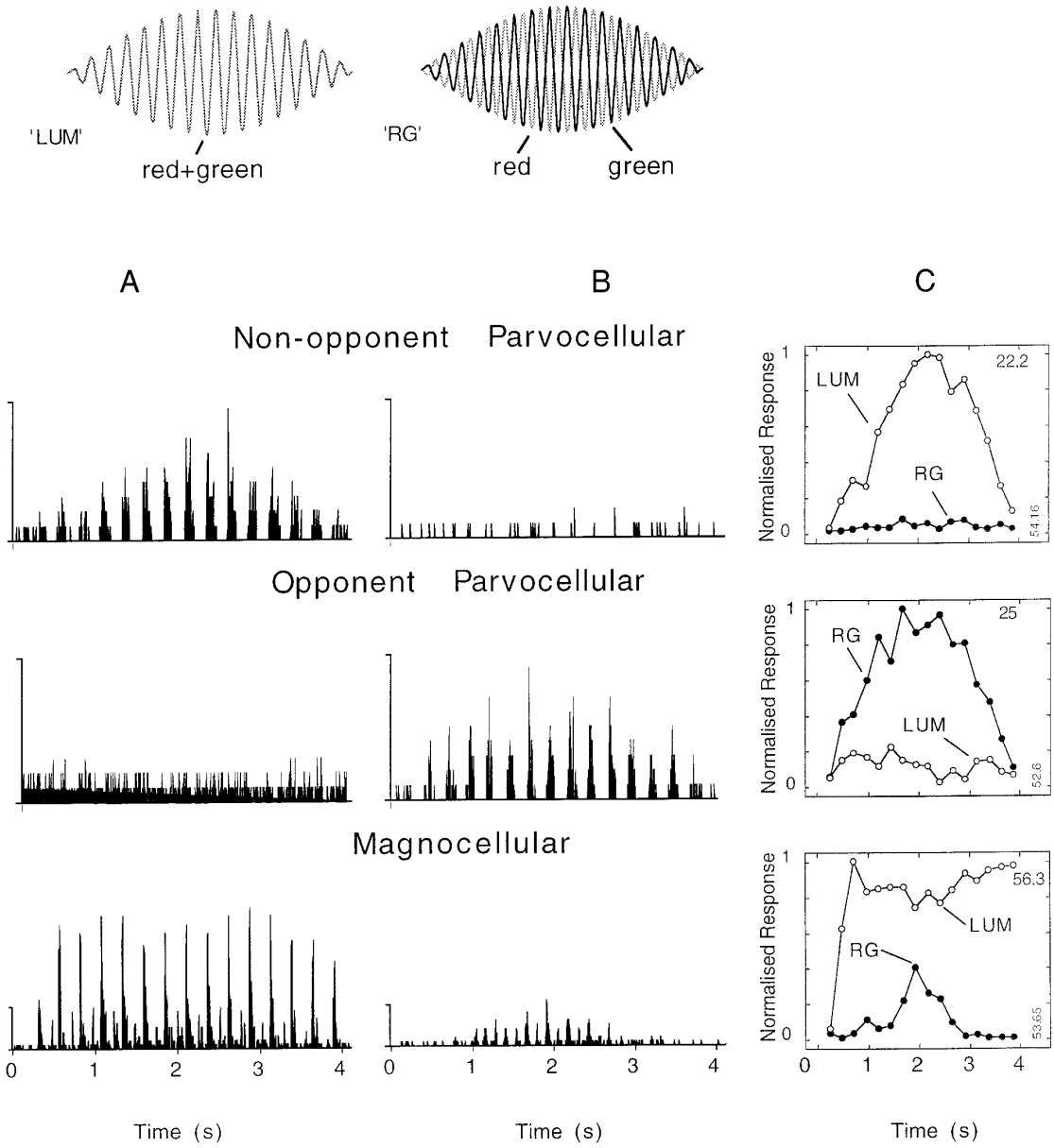

FIG. 7. Responses of different cell types in the LGN to contrast varying stimuli modulated at 3.906 Hz. Each row shows the responses of a different cell to two different stimulus paradigms; in-phase (LUM, *A*) or out of phase (RG, *B*) modulation of luminance matched red and green LEDs. The stimulus contrast was modulated with a sine wave envelope over a 4.1-s epoch. Average peristimulus histograms for 16 stimulus presentations are shown. Vertical scale 20 impulses/s. *C*: amplitude of the 3.906-Hz Fourier component of the cell's response for each stimulus is compared. The significant response to chromatic modulation defines the opponent PC cell. The MC cell shows greater achromatic contrast sensitivity than the PC cell.

held stimuli. As for blue-ON cells in macaque LGN (Derrington et al. 1984) and retina (Lee et al. 1989b; Yeh et al. 1995b), these cells are sensitive to stimuli designed to modulate, selectively, the SWS cones (Fig. 9*A*). The response to in-phase modulation of the red and green diodes (Fig. 9*B*) is of comparable amplitude and opposite phase to the response to SWS cone modulation (Fig. 9, *C*–*E*). Responses to the SWS isolating stimulus were not seen in nonopponent PC cells (Fig. 9*F*), other interlaminar zone cells (Fig. 9*G*), or ML opponent PC cells (data not shown). The majority of MC cells showed no response (Fig. 9*H*). Some MC cells with very high sensitivity to luminance contrast did show some response to SWS modulation, but it is likely to be due to a residual luminance component in the stimulus because, for ON-center cells, the response to SWS modulation had the same phase as the response to luminance modulation.

Figure 10*A* compares the laminar position of 13 blue-ON cells with that of ML opponent cells. Although the interlaminar zones make up a much smaller proportion of the LGN than do the PC layers, the majority of blue-ON cells is located there. By contrast, cells that display ML opponent behavior are confined to the PC laminae (Fig. 10*B*). This result extends the result of Martin et al. (1997) that blue-ON cells are segregated to the interlaminar zones, by showing that ML responses are likewise segregated, but the segregation is to the main PC layers.

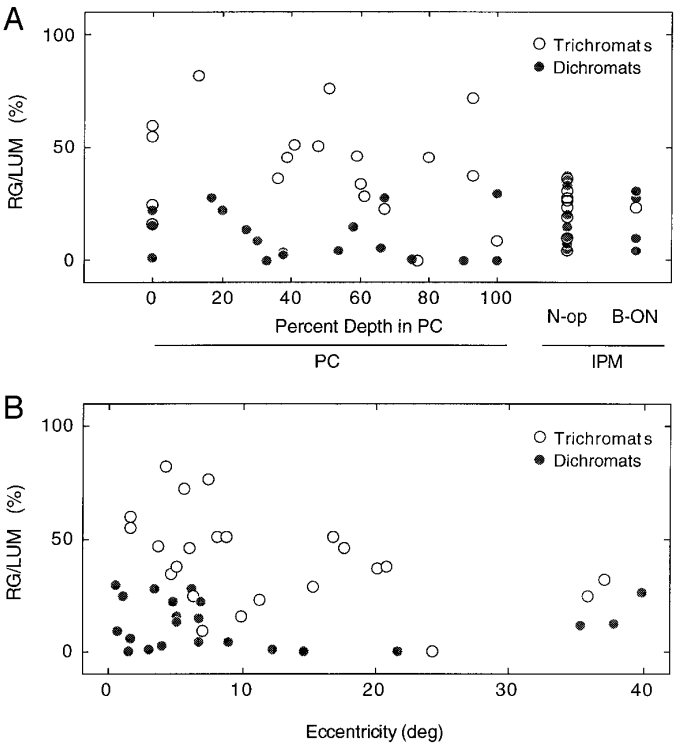

FIG. 8. *A*: distribution of ML opponent responses in the PC layers (PC) and interlaminar zone (IPM). Each point shows the relative response amplitude for luminance (LUM) and red–green chromatic (RG) stimuli as a function of cell position relative to the borders of the internal or external PC lamina. Open circles, trichromats; closed circles, dichromats. RG opponent cells in trichromats are distributed throughout the PC layers. In the interlaminar zone, both blue-ON (B-ON) and other cells (N-op) show relatively poor responses to RG modulation. *B*: data from PC cells are plotted as a function of receptive field eccentricity. Nearly all the cells that show RG opponent response have receptive fields located ≤10° of the fovea.

DISCUSSION

Visual field representation and retinal topography

Our results show that over one-third of the volume of the marmoset LGN is devoted to the representation of the central 5° of the visual field. As Table 1 shows, this central magnification is at least as great as that reported for macaque (Connolly and van Essen 1984; Malpeli and Baker 1975; Malpeli et al. 1996). Two other shared features are apparent. First, in both species the ratio of PC to MC volume is similar (marmoset, 3:1; macaque, 4.1:1, Table 1). Second, the PC:MC ratio is slightly higher in the central 5° than outside. Our results cannot address directly the controversial issue of whether the ratio of PC to MC cells decreases with eccentricity (Ahmad and Spear 1993; Connolly and van Essen 1984; Livingstone and Hubel 1988; Malpeli et al. 1996; Schein and De Monasterio 1987), but we note (Table 1) that the marmoset LGN does not show the kind of decrease calculated for macaque (Connolly and Van Essen 1984; Malpeli et al. 1996).

The dominance of the central visual field representation is associated with the presence of a fovea in both marmoset and macaque (Rohen and Castenholz 1967; Walls 1953; Wilder et al. 1996), but it is not evident in afoveate primates (reviewed by Casagrande and Norton 1991). Ganglion cell density and foveal cone topography are similar in macaque and marmoset (Schein 1988; Troilo et al. 1993; Wässle et al. 1989; Wilder et al. 1996), suggesting that the large volume of LGN devoted to the fovea serves to allow precise connectivity between retinal ganglion cells and geniculocortical relay cells (Conley and Fitzpatrick 1989; Spear et al. 1996; Walls 1953). This is all consistent with the hypothesis that the presence of a fovea is a necessary condition for trichromacy in primates. Accordingly, all the afoveate primate species whose color vision was studied are either dichromats or monochromats (reviewed by Jacobs 1993).

Segregation of response properties in the PC layers

In macaque, ON-center responses are at least partially localized to the two external PC layers (Derrington and Lennie 1984; Kaplan and Shapley 1986; Schiller and Colby 1983; Schiller and Malpeli 1978; Wiesel and Hubel 1966). This finding can be reconciled with our results if one accepts that the two internal PC layers in macaque are each functionally equivalent to the internal aspect of one PC layer in marmoset. Furthermore, a parallel can be drawn with other mammals in which there is a clear segregation of ON and OFF responses within the LGN [mink (Le Vay and McConnell 1982), ferret (Stryker and Zahs 1983), and tree shrew (Conway and Schiller 1983; Holdefer and Norton 1995)]. For all these species, as for primates, the ON responses are segregated furthest from the optic tract for each eye's territory in the LGN. This segregation is independent of the chromatic phenotype of the animal.

Unlike ON and OFF responses, red–green opponent (ML) responses in trichromatic animals were not segregated according to depth within the PC laminae. However, the ML opponent cells encountered all had receptive fields ≤16° of the fovea. Although our sample of ML opponent cells is small, the results are consistent with the hypothesis that the generation of ML opponent responses depends on the precise connectivity among cones, midget bipolar cells, and midget ganglion cells, which is specific to the central retina in primates.

The existence of a high proportion of nonopponent PC cells in trichromatic marmosets (Yeh et al. 1995b; this study) was unexpected given that similar (large field; low spatial frequency dominated) stimuli reveal opponent behavior in the majority of PC pathway cells in macaque retina and LGN (De Monasterio et al. 1975; Derrington et al. 1984; Padmos and Van Norren 1975). The low proportion of ML opponent cells in marmoset could arise because the density of cones in the perifoveal retina of marmoset is higher than that for macaque (Goodchild et al. 1996). For example, between 10 and 15° from the fovea, the numerical convergence of cones to midget cells for macaque is <5:1 but for marmoset is over 30:1 (Goodchild et al. 1996). Accordingly, mathematical simulations (De Valois and De Valois 1993; Lennie et al. 1991; Paulus and Kröger-Paulus 1983) show that the proportion of ML opponent cells should decrease with increasing convergence if the opponent cells draw their input indiscriminately from the local ML cone array. Recent in vitro studies of midget ganglion cells in the far peripheral retina in macaque (Dacey 1994; Dacey and Lee 1997) likewise show that reduced ML opponency is present where cone convergence is greater.

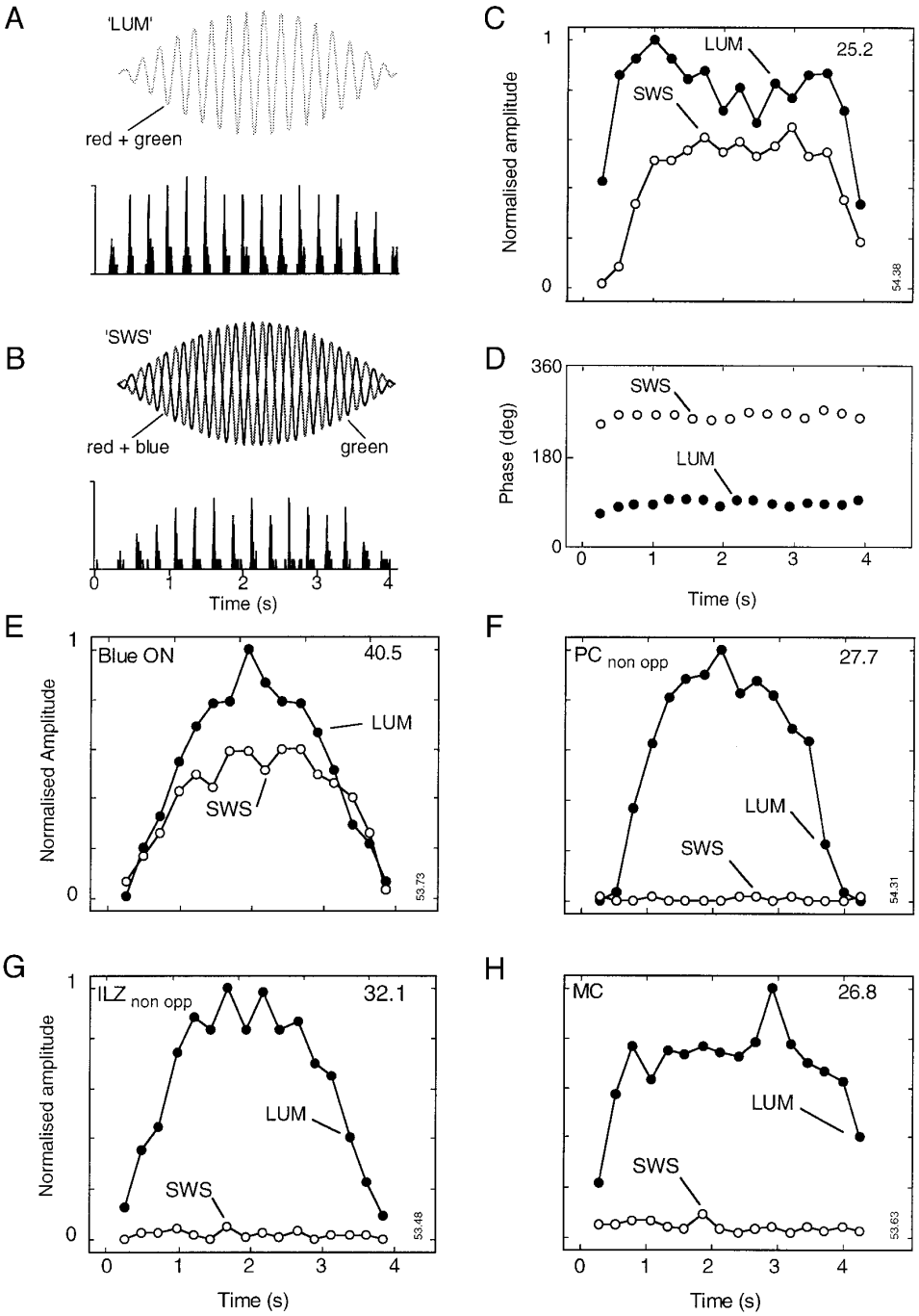

FIG. 9. Responses of cells to short-wavelength sensitive (SWS) isolating stimulus. *A* and *B*: blue-ON cell. The stimulus waveform is sketched above peristimulus time histograms for (*A*) in-phase modulation of red and green LEDs (LUM) and (*B*) SWS cone isolating stimulus. Vertical scale, 10 impulses/sec. *C* and *D*: amplitude (*C*) and phase (*D*) of the 3.906-Hz Fourier component of the cell response to each stimulus. The cell shows contrast-dependent responses to both stimuli at opposite phase to SWS (blue-ON) and LUM (yellow-OFF). *E–G*: responses of other cells to these stimuli. Amplitude values shown as in *C*. Blue-ON cells (*E*) always respond to the SWS stimulus, but there is no response to the SWS stimulus for the majority of nonopponent (*F*) PC cells, of interlaminar zone (*G*) cells. MC cells (*H*) respond vigorously to luminance contrast but show little or no response to SWS modulation.

Interlaminar zone

The interlaminar zone in marmoset is probably functionally equivalent to the intercalated layers in macaque and other simian primates and to the koniocellular layers in the nocturnal prosimian *Galago* (for reviews see Casagrande 1994; Casagrande and Norton 1991). Our finding that SWS opponent signals are segregated to the interlaminar zone (Martin et al. 1997; this study) is likewise consistent with recent evidence that blue-ON responses are segregated to the interlaminar zones in the macaque (Reid et al. 1997) and add to the evidence for a distinct pathway for SWS cone signals within the retina (Dacey and Lee 1994; Ghosh et al. 1997; Kouyama and Marshak 1992) and central visual pathways of primates. Our results suggest that only a small proportion of interlaminar zone cells are blue-ON cells, but we did not study systematically the properties of the other (nonopponent) cell types, except to confirm that the visuotopic map in the interlaminar zone is in broad register with that of the main PC and MC layers. Nevertheless, our qualitative assessment of the receptive fields of interlaminar zone cells clearly indicated that, as for koniocellular cells in the nocturnal prosimian *Galago* (Norton and Casagrande 1982), the interlaminar zone cells in marmoset show a wide variety of response properties. More recent anatomic data likewise suggest that there may be morphological and neurochemical

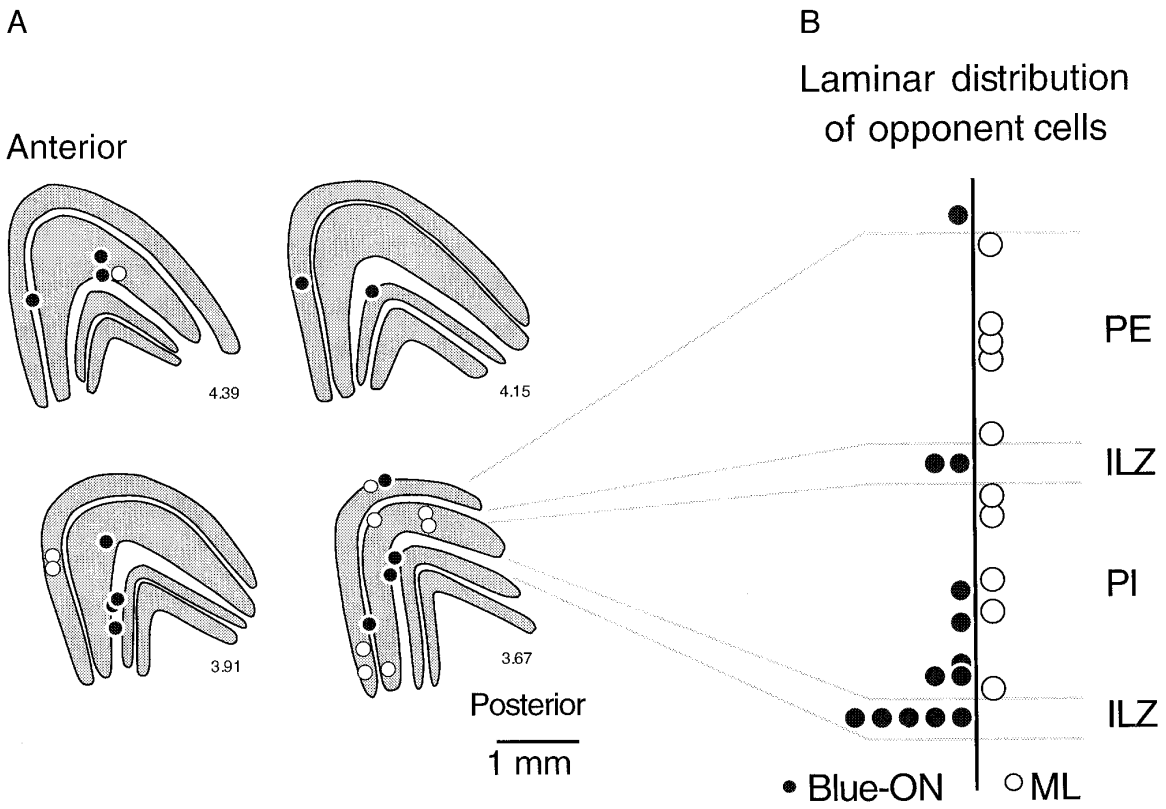

FIG. 10. *A*: outline drawings of coronal sections at 4 levels through the posterior one-half of the marmoset LGN, showing the location of blue-ON cells (●) and ML opponent cells (○). Results pooled from 4 animals. The majority of blue-ON cells is located in the interlaminar zone between the MC and PC laminae. *B*: comparison of the intralaminar location of blue-ON cells with ML opponent cells. The location of each recorded cell with respect to the laminar borders is shown as a histogram. Blue-ON cells are segregated to the interlaminar zones and the internal border of the internal PC layer, but ML opponent responses are distributed throughout the PC layers. Abbreviations as for Fig. 1.

heterogeneity in the koniocellular pathway in *Galago* (Ding and Casagrande 1997) and marmoset (Goodchild and Martin 1998). That the interlaminar/koniocellular division of the LGN in marmoset is anatomically segregated from the PC layers enabled the blue-ON cells to be assigned with confidence to the koniocellular pathway in this study and give promise that other functional subgroups of cells in the ''third geniculocortical pathway'' (Casagrande 1994; Hendry and Yoshioka 1994) can be delineated in this species.

We thank R. Phillips and A. Lara for technical assistance and J. Potas for assistance with the LGN reconstructions; J. Kremers, T. Yeh, B. B. Lee, and U. Grünert for helpful comments and discussion; and Dr. Sander Beckers and Abbot Australasia for the kind donation of isofluorane used in these experiments.

This work was supported by National Health and Medical Research Council of Australia Grant 096070.

Address for reprint requests: P. R. Martin, Dept. Physiology F13, University of Sydney, NSW 2006, Australia.

Received 5 January 1998; accepted in final form 1 July 1998.

REFERENCES

AHMAD, A. AND SPEAR, P. D. Effects of aging on the size, density, and number of rhesus monkey lateral geniculate neurons. *J. Comp. Neurol.* 334: 631–643, 1993.

BISHOP, P. O., BURKE, W., AND DAVIS, R. The interpretation of the extracellular response of lateral geniculate cells. *J. Physiol. (Lond.)* 162: 451–472, 1962.

BLAKEMORE, C. AND VITAL-DURAND, F. Organization and post-natal development of the monkey's lateral geniculate nucleus. *J. Physiol. (Lond.)* 380: 453–491, 1986.

CASAGRANDE, V. A. A third parallel visual pathway to primate area V1. *Trends Neurosci.* 17: 305–310, 1994.

CASAGRANDE, V. A. AND NORTON, T. T. Lateral geniculate nucleus: a review of its physiology and function. In: *The Neural Basis of Visual Function*, edited by A. G. Leventhal. New York: Macmillan, 1991, p. 41–84.

CONLEY, M. AND FITZPATRICK, D. Morphology of retinogeniculate axons in the macaque. *Vis. Neurosci.* 2: 287–296, 1989.

CONNOLLY, M. AND VAN ESSEN, D. The representation of the visual field in parvicellular and magnocellular layers of the lateral geniculate nucleus of the macaque monkey. *J. Comp. Neurol.* 226: 544–564, 1984.

CONWAY, J. L. AND SCHILLER, P. H. Laminar organization of tree shrew dorsal lateral geniculate nucleus. *J. Neurophysiol.* 50: 1330–1342, 1983.

CURCIO, C. A., SLOAN, K. R., KALINA, R. E., AND HENDRICKSON, A. E. Human photoreceptor topography. *J. Comp. Neurol.* 292: 497–523, 1990.

DACEY, D. M. Physiology, morphology and spatial densities of identified ganglion cell types in primate retina. In: *Higher Order Processing in the Visual System*. *Ciba Foundation Symposium 184*, edited by G. R. Bock and J. A. Goode. Chichester: Wiley, 1994.

DACEY, D. M. AND LEE, B. B. The ''blue-on'' opponent pathway in primate retina originates from a distinct bistratified ganglion cell type. *Nature* 367: 731–735, 1994.

DACEY, D. M. AND LEE, B. B. Cone inputs to the receptive field of midget ganglion cells in the periphery of macaque retina. *Invest. Ophthalmol.* 38: S708, 1997.

DE MONASTERIO, F. M., GOURAS, P., AND TOLHURST, D. J. Concealed colour opponency in ganglion cells of the rhesus monkey retina. *J. Physiol. (Lond.)* 251: 217–229, 1975.

DERRINGTON, A. M., KRAUSKOPF, J., AND LENNIE, P. Chromatic mechanisms in lateral geniculate nucleus of macaque. *J. Physiol. (Lond.)* 357: 241–265, 1984.

DERRINGTON, A. M. AND LENNIE, P. Spatial and temporal contrast sensitivities of neurones in lateral geniculate nucleus of macaque. *J. Physiol. (Lond.)* 357: 219–240, 1984.

DE VALOIS, R. L. AND DE VALOIS, K. K. A multi-stage color model. *Vision Res.* 33: 1053–1065, 1993.

DING, Y. AND CASAGRANDE, V. A. The distribution and morphology of LGN K pathway axons within the layers and CO blobs of owl monkey V1. *Vis. Neurosci.* 14: 691–704, 1997.

DREHER, B., FUKADA, Y., AND RODIECK, R. W. Identification, classification and anatomical segregation of cells with X-like and Y-like properties in the lateral geniculate nucleus of Old-World primates. *J. Physiol. (Lond.)* 258: 433–452, 1976.

GHOSH, K. K., GOODCHILD, A. K., SEFTON, A. E., AND MARTIN, P. R. Morphology of retinal ganglion cells in a new world monkey, the marmoset *Callithrix jacchus*. *J. Comp. Neurol.* 366: 76–92, 1996.

GHOSH, K. K., MARTIN, P. R., AND GRÜNERT, U. Morphological analysis of the blue cone pathway in the retina of a new world monkey, the marmoset *Callithrix jacchus*. *J. Comp. Neurol.* 379: 211–225, 1997.

GOODCHILD, A. K., GHOSH, K. K., AND MARTIN, P. R. Comparison of photoreceptor spatial density and ganglion cell morphology in the retina of human, macaque monkey, cat, and the marmoset *Callithrix jacchus*. *J. Comp. Neurol.* 366: 55–75, 1996.

GOODCHILD, A. K. AND MARTIN, P. R. The distribution of calcium binding proteins in the lateral geniculate nucleus and visual cortex of a New World monkey, the marmoset *Callithrix jacchus*. *Visual Neurosci.* 15: 625–641, 1998.

GUNDERSEN, H.J.G. AND JENSEN, E. B. The efficiency of systematic sampling in stereology and its prediction. *J. Microsc.* 147: 229–263, 1987.

HENDRY, S.H.C. AND YOSHIOKA, T. A neurochemically distinct third channel in the macaque dorsal lateral geniculate nucleus. *Science* 264: 575–577, 1994.

HICKS, T. P., LEE, B. B., AND VIDYASAGAR, T. R. The responses of cells in macaque lateral geniculate nucleus to sinusoidal gratings. *J. Physiol. (Lond.)* 337: 183–200, 1983.

HOLDEFER, R. N. AND NORTON, T. T. Laminar organization of receptive field properties in the dorsal lateral geniculate nucleus of the tree shrew (*Tupaiaglis belangeri*). *J. Comp. Neurol.* 358: 401–413, 1995.

HUNT, D. M., WILLIAMS, A. J., BOWMAKER, J. K., AND MOLLON, J. D. Structure and evolution of the polymorphic photopigment gene of the marmoset. *Vision Res.* 33: 147–154, 1993.

JACOBS, G. H. Differences in spectral response properties of LGN cells in male and female squirrel monkeys. *Vision Res.* 23: 461–468, 1983.

JACOBS, G. H. The distribution and nature of colour vision among the mammals. *Biol. Rev.* 68: 413–471, 1993.

JACOBS, G. H. Primate photopigments and primate color vision. *Proc. Natl. Acad. Sci. USA* 93: 577–581, 1996.

JACOBS, G. H., NEITZ, M., DEEGAN, J. F., AND NEITZ, J. Trichromatic colour vision in new world monkeys. *Nature* 382: 156–158, 1996.

KAAS, J. H., HUERTA, M. F., WEBER, J. T., AND HARTING, J. K. Patterns of retinal terminations and laminar organization of the lateral geniculate nucleus of primates. *J. Comp. Neurol.* 182: 517–554, 1978.

KAPLAN, E. AND SHAPLEY, R. M. The primate retina contains two types of ganglion cells, with high and low contrast sensitivity. *Proc. Natl. Acad. Sci. USA* 83: 2755–2757, 1986.

KOUYAMA, N. AND MARSHAK, D. W. Bipolar cells specific for blue cones in the macaque retina. *J. Neurosci.* 12: 1233–1252, 1992.

KREMERS, J., WEISS, S., AND ZRENNER, E. Temporal properties of marmoset lateral geniculate cells. *Vision Res.* 37: 2649–2660, 1997.

KREMERS, J., WEISS, S., ZRENNER, E., AND MAURER, J. Rod and cone inputs to parvo- and magnocellular cells in the dichromatic common marmoset (*Callithrix Jacchus*). In: *Colour Vision Deficiencies*, edited by C. R. Cavonius. Dordrecht: Kluwer, 1997, p. 87–97.

LE GROS CLARK, W. E. The laminar organization and cell content of the lateral geniculate body in the monkey. *J. Anat.* 75: 419–433, 1941.

LE VAY, S. AND MCCONNELL, S. K. ON and OFF layers in the lateral geniculate nucleus of the mink. *Nature* 300: 350–351, 1982.

LEE, B. B., MARTIN, P. R., AND VALBERG, A. Nonlinear summation of M- and L-cone inputs to phasic retinal ganglion cells of the macaque. *J. Neurosci.* 9: 1433–1442, 1989a.

LEE, B. B., MARTIN, P. R., AND VALBERG, A. Sensitivity of macaque retinal ganglion cells to chromatic and luminance flicker. *J. Physiol. (Lond.)* 414: 223–243, 1989b.

LENNIE, P., HAAKE, P. W., AND WILLIAMS, D. R. The design of chromatically opponent receptive fields. In: *Computational Models of Visual Processing*, edited by M. S. Landy and J. A. Movshon. Cambridge, MA: MIT Press, 1991, p. 71–82.

LIVINGSTONE, M. S. AND HUBEL, D. H. Do the relative mapping densities of the magno- and parvocellular systems vary with eccentricity? *J. Neurosci.* 8: 4334–4339, 1988.

MALPELI, J. G. AND BAKER, F. H. The representation of the visual field in the lateral geniculate nucleus of *Macaca mulatta*. *J. Comp. Neurol.* 161: 569–594, 1975.

MALPELI, J. G., LEE, D., AND BAKER, F. H. Laminar and retinotopic organization of the macaque lateral geniculate nucleus: magnocellular and parvocellular magnification functions. *J. Comp. Neurol.* 375: 363–377, 1996.

MARTIN, P. R., WHITE, A. J., GOODCHILD, A. K., WILDER, H. D., AND SEFTON, A. E. Evidence that blue-on cells are part of the third geniculocortical pathway in primates. *Eur. J. Neurosci.* 9: 1536–1541, 1997.

MOLLON, J. D., BOWMAKER, J. K., AND JACOBS, G. H. Variations of colour vision in a New World primate can be explained by polymorphism of retinal photopigments. *Proc. R. Soc. Lond. B. Biol. Sci.* 222: 373–399, 1984.

NORTON, T. T. AND CASAGRANDE, V. A. Laminar organization of receptive-field properties in lateral geniculate nucleus of bush baby (*Galago crassicaudatus*). *J. Neurophysiol.* 47: 715–741, 1982.

PADMOS, P. AND VAN NORREN, D. Cone systems interaction in single neurons of the lateral geniculate nucleus of the macaque. *Vision Res.* 15: 617–619, 1975.

PAULUS, W. AND KRÖGER-PAULUS, A. A new concept of retinal colour coding. *Vision Res.* 23: 529–540, 1983.

REID, R. C., ALONSO, J.-M., AND HENDRY, S.H.C. S-cone input is relayed to visual cortex from two koniocellular layers of macaque LGN. *Soc. Neurosci. Abstr.* 23: 13, 1997.

ROHEN, J. W. AND CASTENHOLZ, A. Über die Zentralisation der Retina bei Primaten. *Folia Primatol. (Basel)* 5: 92–147, 1967.

SCHEIN, S. J. Anatomy of macaque fovea and spatial densities of neurons in foveal representation. *J. Comp. Neurol.* 269: 479–505, 1988.

SCHEIN, S. J. AND DE MONASTERIO, F. M. Mapping of retinal and geniculate neurons onto striate cortex of macaque. *J. Neurosci.* 7: 996–1009, 1987.

SCHILLER, P. H. AND COLBY, C. L. The responses of single cells in the lateral geniculate nucleus of the rhesus monkey to color and luminance contrast. *Vision Res.* 23: 1631–1641, 1983.

SCHILLER, P. H. AND MALPELI, J. G. Functional specificity of lateral geniculate nucleus laminae of the rhesus monkey. *J. Neurophysiol.* 41: 788–797, 1978.

SMITH, V. C., LEE, B. B., POKORNY, J., MARTIN, P. R., AND VALBERG, A. Responses of macaque ganglion cells to the relative phase of heterochromatically modulated lights. *J. Physiol. (Lond.)* 458: 191–221, 1992.

SPATZ, W. B. The retino-geniculo-cortical pathway in *Callithrix* I. Intraspecific variations in the lamination pattern of the lateral geniculate nucleus. *Exp. Brain Res.* 33: 551–563, 1978.

SPEAR, P. D., KIM, C.B.Y., AHMAD, A., AND TOM, B. W. Relationship between numbers of retinal ganglion cells and lateral geniculate neurons in the rhesus monkey. *Visual Neurosci.* 13: 199–203, 1996.

STEPHAN, H., BARON, G., AND SCHWERDTFEGER, W. K. *The Brain of the Common Marmoset (Callithrix jacchus). A Stereotaxic Atlas*. Berlin: Springer-Verlag, 1980.

STRYKER, M. P. AND ZAHS, K. R. ON and OFF sublaminae in the lateral geniculate nucleus of the ferret. *J. Neurosci.* 3: 1943–1951, 1983.

SWANSON, W. H., POKORNY, J., AND SMITH, V. C. Effects of temporal frequency on phase-dependent sensitivity to heterochromatic flicker. *J. Opt. Soc. Am. A* 4: 2266–2273, 1987.

TOVÉE, M. J., BOWMAKER, J. K., AND MOLLON, J. D. The relationship between cone pigments and behavioural sensitivity in a New World monkey *(Callithrix jacchus jacchus)*. *Vision Res.* 32: 867–878, 1992.

TRAVIS, D. S., BOWMAKER, J. K., AND MOLLON, J. D. Polymorphism of visual pigments in a callitrichid monkey. *Vision Res.* 28: 481–490, 1988.

TROILO, D., HOWLAND, H. C., AND JUDGE, S. J. Visual optics and retinal cone topography in the common marmoset *(Callithrix jacchus)*. *Vision Res.* 33: 1301–1310, 1993.

WALLS, G. L. The lateral geniculate nucleus and visual histophysiology. Berkeley, CA: University of California Publications in Physiology, 1953, vol. 9, p. 1–100.

WÄSSLE, H. AND BOYCOTT, B. B. Functional architecture of the mammalian retina. *Physiol. Rev.* 71: 447–480, 1991.

WÄSSLE, H., GRÜNERT, U., RÖHRENBECK, J., AND BOYCOTT, B. B. Cortical magnification factor and the ganglion cell density of the primate retina. *Nature* 341: 643–646, 1989.

WESTHEIMER, G. The Maxwellian view. *Vision Res.* 6: 669–682, 1966.

WIESEL, T. N. AND HUBEL, D. H. Spatial and chromatic interactions in the lateral geniculate body of the rhesus monkey. *J. Neurophysiol.* 29: 1115–1156, 1966.

WILDER, H., GRÜNERT, U., LEE, B. B., AND MARTIN, P. R. Topography of ganglion cells and photoreceptors in the retina of a New World monkey: the marmoset *Callithrix jacchus*. *Visual Neurosci.* 13: 335–352, 1996.

WILLIAMS, A. J., HUNT, D. M., BOWMAKER, J. K., AND MOLLON, J. D. The polymorphic photopigments of the marmoset: spectral tuning and genetic basis. *EMBO J.* 11: 2039–2045, 1992.

YAMADA, E. S., SILVEIRA, L.C.L., GOMES, F. L., AND LEE, B. B. The retinal ganglion cell classes of new world primates. *Rev. Bras. Biol.* 56: 381–396, 1996.

YEH, T., LEE, B. B., AND KREMERS, J. Temporal response of ganglion cells of the macaque retina to cone-specific modulation. *J. Opt. Soc. Am. A* 12: 456–464, 1995a.

YEH, T., LEE, B. B., KREMERS, J., COWING, J. A., HUNT, D. M., MARTIN, P. R., AND TROY, J. B. Visual responses in the lateral geniculate nucleus of dichromatic and trichromatic marmosets *(Callithrix jacchus)*. *J. Neurosci.* 15: 7892–7904, 1995b.